

Article

Hydrological Change Detection and Process Simulation for a Semi-Arid Catchment in Northern China

Yue Liu ^{1,2,3}, Jianyun Zhang ^{1,2,3,4}, Zhenxin Bao ^{3,4} , Yanqing Yang ^{3,4,5} and Guoqing Wang ^{2,3,4,*} 

- ¹ College of Hydrology and Water Resources, Hohai University, Nanjing 210098, China; liuyue_hhu@163.com (Y.L.); jyzhang@nhri.cn (J.Z.)
- ² Yangtze Institute for Conservation and Development, Nanjing 210098, China
- ³ Research Center for Climate Change, Ministry of Water Resources, Nanjing 210029, China; zxbao@nhri.cn (Z.B.); 2017323060018@stu.scu.edu.cn (Y.Y.)
- ⁴ State Key Laboratory of Hydrology—Water Resources and Hydraulic Engineering, Nanjing Hydraulic Research Institute, Nanjing 210029, China
- ⁵ State Key Laboratory of Hydraulics and Mountain River Engineering, College of Water Resource and Hydropower, Sichuan University, Chengdu 610065, China
- * Correspondence: gqwang@nhri.cn; Tel.: +86-25-8582-8531

Abstract: In-depth understanding and accurate simulation of hydrological processes are of great significance for sustainable development and management of water resources. The study focused on a semi-arid catchment, the upper Tang River catchment in northern China, and investigated the performance of the RCCC-WBM model based on the detection results of trend, mutation, and periodicity. Results show that (1) as a result of climate change and intensive human activities, the observed runoff series after TFPW (trend-free pre-whiting) pretreatment presented a significant downward trend with the mutation point in 1996; (2) the abrupt change of air temperature series was also in 1996 with a significant rising trend, while the annual precipitation series exhibited an insignificant declining trend with no obvious mutation during 1973–2014; (3) the precipitation and runoff series had periodic variations roughly 7a multiples with the periodic oscillation strongest around 14a, while the air temperature series showed only one dominant period of 28a; (4) the RCCC-WBM model performed well in discharge simulation before the mutation year but gradually lost its stability after 1996, which was mainly affected by anthropogenic activities. It is essential to accurately identify the characteristics of hydrological elements and improve the applicability of hydrological models in the changing environment in future studies.

Keywords: the upper Tang River catchment; interannual variability; wavelet analysis; the RCCC-WBM model; human activities



Citation: Liu, Y.; Zhang, J.; Bao, Z.; Yang, Y.; Wang, G. Hydrological Change Detection and Process Simulation for a Semi-Arid Catchment in Northern China. *Water* **2022**, *14*, 1267. <https://doi.org/10.3390/w14081267>

Academic Editor: Aizhong Ye

Received: 9 March 2022

Accepted: 11 April 2022

Published: 13 April 2022

Publisher's Note: MDPI stays neutral with regard to jurisdictional claims in published maps and institutional affiliations.



Copyright: © 2022 by the authors. Licensee MDPI, Basel, Switzerland. This article is an open access article distributed under the terms and conditions of the Creative Commons Attribution (CC BY) license (<https://creativecommons.org/licenses/by/4.0/>).

1. Introduction

The evolution characteristics and laws of hydrometeorological series under the changing environment are an essential part of the “Panta Rhei—Everything Flows” project (2013–2022) [1]. In recent years, climate change and human activities, such as water conservancy projects, groundwater overexploitation, and urbanization construction, have not only significantly altered the physical mechanism of hydrological cycle [2,3] but also brought unprecedented challenges to the application of hydrological models [4,5]. Therefore, accurately identifying the inconsistencies of hydrological series and selecting appropriate hydrological models for runoff simulation are of scientific significance for sustainable management and utilization of water resources in the catchment, especially in arid and semi-arid water-deficient regions [6].

The inconsistencies of hydrological and meteorological series are mainly manifested in trend, mutation, and periodicity. The trend test methods include Correlation Coefficient, Mann–Kendall test, and Hurst Coefficient [7,8]. The mutation test methods are generally

divided into parametric ones and non-parametric ones. The non-parametric methods are more suitable for mutation test of hydrometeorological series since they are not disturbed by a few outliers [9], mainly including Pettitt test, Mann–Kendall test, and Spearman's rho test [10,11]. The periodicity test, wavelet analysis, variance analysis, and power spectrum analysis are effective methods that have been commonly used [12]. It is worth noting that the autocorrelation of the series should not be ignored in the analysis, otherwise the accuracy of the detected characteristics will be affected [13]. As a typical de-trending method, the trend-free pre-whiting (TFPW) has been widely applied in precipitation, runoff, temperature, evaporation, and drought index [14–16]. Mallick et al. [17] used TFPW and Mann–Kendall methods to explore annual rainfall variabilities and trends in Asir region and provided planners and policymakers with a basis for decision-making on water management. Liu et al. [18] combined the TFPW into an elasticity method to explore the sensitivity of crop yields to climate variables and complemented existing linear models for detecting the response of crop yields to climate change.

Hydrological models have been an essential tool for understanding water cycle processes by simulating complex hydrological systems through mathematical methods and played an important role in flow forecasting, water resources management, and climate change impact analysis [19,20]. The simulation of the water cycle process in arid and semi-arid regions has always been a hot issue in hydrological research. Previous studies have shown that most hydrological models perform less well in arid and semi-arid regions than in other climate regions due to frequent human activities and water shortage [21]. Zoccatelli et al. [22] characterized the conditions where models fail systematically in desert areas of the eastern Mediterranean and presented an analysis of the model setting to deepen the understanding of errors. Hosseini and Khaleghi [23] evaluated the SWAT model performance of sediment flow simulations and investigated the model uncertainties for arid and semi-arid catchments. So far, the application of hydrological models has mainly focused on flow simulation in natural periods [24]. However, intensive human activities not only destroy the consistency of hydrological elements [25] but also make the nonlinear characteristics of surface yield and confluence more obvious [26], which brings a lot of challenges and uncertainties to hydrological modeling, particularly in arid and semi-arid regions [27].

Due to the limited water resources with uneven distribution, the fragile ecological environment in arid and semi-arid regions is more sensitive to climate change and human activities than in other regions [28,29]. Since the 1950s, the observed discharge in most rivers of northern China has been decreasing, especially in the Haihe River, where the contradiction between water supply and demand has become increasingly prominent [30]. The Haihe River is the largest water system in northern China with arable land and population accounting for 8% and 10% of the country, respectively, but water resources only account for 1.3% [31]. Bao et al. [32] investigated the independent driving effects of four factors of air temperature, precipitation, underlying surface, and water withdrawal on runoff reduction in the Haihe River basin, and found that anthropogenic impacts played a dominant role in runoff decrease, accounting for 62%–68% of the total reduction, among which water withdrawal was the most significant factor (about 55%).

The upper Tang River catchment, located in the middle of the Haihe River basin, was chosen as the research object in this paper. The main objectives of this research are as follows: (1) to systematically identify climate change in this study catchment and inconsistencies of the observed runoff series under the changing environment; (2) to test the performance and applicability of the RCCC-WBM model under the influence of human activities in semi-arid regions; (3) to provide a scientific basis for sustainable management of water resources in northern China by hydrological change detection and modeling.

2. Study Area and Data Sources

The Tang River is a significant part of the Haihe River system, being the upper source of the Daqing River, with a total river length of 273 km and a drainage area of 4990 km². It

originates from Qiangfeng Ridge and flows eastward to Baiyang Lake, crossing 10 cities and counties in Hebei and Shanxi provinces. The Daomaguan hydrometric station ($114^{\circ}38'$ E, $39^{\circ}05'$ N), located in the upper reaches of the Tang River, is in the transitional zone between plains and mountains, covering a drainage area of 2770 km^2 . The terrain of the upper Tang River catchment is dominated by hills and mountains, with the altitude in the northwest higher than that in the southeast. Figure 1 shows the terrain, river network, and geographical location of the hydrometric station. The upper Tang River catchment is in the temperate continental monsoon climate zone with an annual average temperature of 6.6°C . The precipitation of the catchment manifests in an uneven distribution in time and space (with the mean annual value of 520.0 mm), which can easily cause serious droughts and devastating floods. There are no large-scale hydraulic projects in the upper reaches of the Tang River. The main channel has base flow all year round, with an average annual discharge of $5.0 \text{ m}^3/\text{s}$. Agriculture plays an important role in this catchment, with main crops including wheat, corn, and cotton.

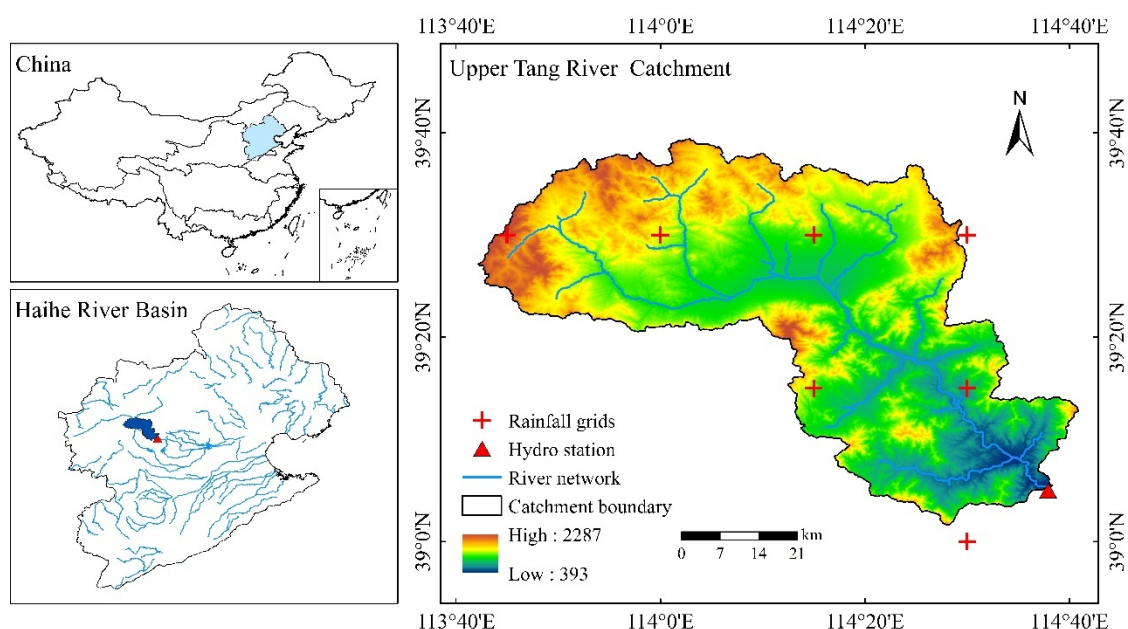


Figure 1. The terrain, river network, and geographical location of the hydrometric station in the upper Tang River catchment.

We take the upper Tang River catchment gauged by the Daomaguan hydrometric station in the Haihe River basin as the research object. The daily hydrological data during 1973–2014 were collected from hydrological yearbooks, the hydrometeorological data were extracted from CMA (China Meteorological Administration), and the DEM elevation data were collected from the ASTER GDEM data set.

3. Methodologies

3.1. Trend-Free Pre-Whiting

The trend-free pre-whiting (TFPW) is an effective method to eliminate the influence of hydrological series trend on autocorrelation coefficient, which can effectively improve the accuracy of the series mutation test [33]. To compute the TFPW of a series X_t , ($t = 1, 2, \dots, n$; n is the length of the series), calculation formulas are as follows:

$$\beta = \text{Median} \left(\frac{X_j - X_i}{j - i} \right), \forall i < j \quad (1)$$

$$Y_t = X_t - \beta t \quad (2)$$

$$Y'_t = Y_t - r Y_{t-1} \tag{3}$$

$$Y''_t = Y'_t + \beta t \tag{4}$$

where β is the linear trend of the series, Y_t is the series after removing the trend, Y'_t is the series after removing serial correlation, Y''_t is the new series after TFPW, and r is the first-order autocorrelation coefficient of Y_t . What should be noted is that when r is small enough, Y_t can be considered as an independent series to be tested for mutations directly without preprocessing.

3.2. Mann–Kendall Method

The MK (Mann–Kendall) method, proposed by Mann [34] and Kendall [35], is non-parametric and has been extensively used in hydrological and meteorological series tests [36]. The MK method is simple to calculate and can detect both sequence trends and mutation points. The Mann–Kendall standardized statistic Z_{MK} is defined to describe the increase or decrease of the time series [37]. A positive value of Z_{MK} means that the series is trending upward, while a negative one represents a downward trend [38]. If Z_{MK} is more than the significance level $\alpha = 5\%$ ($Z_{MK} \geq Z_{\alpha/2} = |\pm 1.96|$), then the trend in the series is considered significant.

3.3. Pettitt Test

The Pettitt test is a non-parametric mutation test method proposed by Pettitt [39]. Assume that the hydrological series x_i ($i = 1, 2, \dots, n$) mutates at t . Then take t as the splitting point to segment the series into two parts. Its formulas are as follows:

$$U_{t,n} = U_{t-1,n} + \sum_{i=1}^n \text{sgn}(x_t - x_i) \quad (t = 2, 3, 4, \dots, n) \tag{5}$$

The statistic $K_{t,n}$ corresponding to the possible mutation point t is calculated by Equation (6):

$$K_{t,n} = \max |U_{t,n}|, \quad (1 \leq t \leq n) \tag{6}$$

The significance level is defined by Equation (7):

$$p_t = 2 \exp \frac{-6K_{t,n}^2}{n^3 + n^2} \tag{7}$$

If $p_t \leq 0.05$, then the mutation point is considered to be significant. It is worth noting that this method has good accuracy in the single mutation point test, but it performs poorly in the multi-mutation point test.

3.4. Sequential Cluster Test

The Sequential Cluster test is based on the sum of squared deviations between classes to determine the mutation points [40]. For the hydrological series x_i ($i = 1, 2, \dots, n$), take t as the most likely mutation point to minimize the sum of squared deviations:

$$\min S_n(t) = \min (V_t + V_{n-t}) \quad 2 \leq t \leq n - 1 \tag{8}$$

$$V_t = \sum_{i=1}^t (x_i - \bar{x}_t)^2 \tag{9}$$

$$V_{n-t} = \sum_{i=t+1}^n (x_i - \bar{x}_{n-t})^2 \tag{10}$$

where $S_n(t)$ is the sum of squared deviation, V_t is the sum of squared deviation before t , V_{n-t} is the sum of squared deviation after t , \bar{x}_t is the mean of series before t , and \bar{x}_{n-t} is the mean of series after t .

3.5. Morlet Wavelet Analysis

The Morlet wavelet analysis can reveal various changes in the series and reflect the changing trends of hydrometeorological data on different time scales [41]. Compared with multi-time scale analysis methods, the wavelet analysis has a better balance in both time and frequency domains. The Morlet wavelet formula is shown in Equation (11):

$$\Psi_0(t) = \pi^{-1/4} e^{iw_0t} e^{-t^2/2} \tag{11}$$

where ψ_0 is the wavelet function, w_0 is the dimensionless frequency, t is the time, i is the serial number, π and e are constants.

3.6. RCCC-WBM Model

The RCCC-WBM model is a simplified large-scale model based on the water balance principle, designed by the RCCC team of China (Research Center for Climate Change), which has been applied for regional water resources assessment and runoff changes attribution with good performance [42,43]. By inputting monthly meteorological data (precipitation, temperature, and potential evaporation), the model estimates monthly stream flow with four parameters describing the characteristics of surface flow (K_s), underground flow (K_g), snowmelt (K_{sn}), and soil moisture content (S_{max}) [44]. The structure, as well as the description of the RCCC-WBM model, is shown in Figure 2.

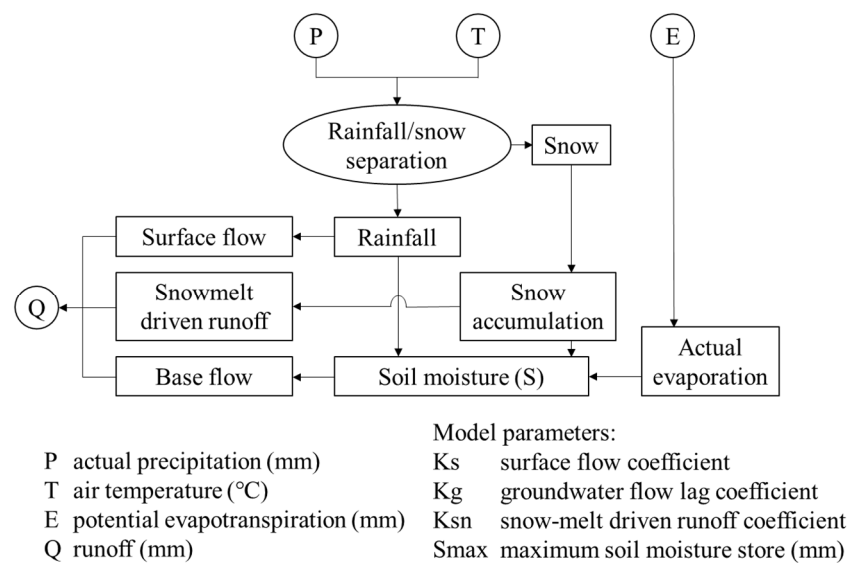


Figure 2. The structure and description of the RCCC-WBM model.

The normalized statistics such as NSE (Nash–Sutcliffe Efficiency) and RE (relative error) are commonly used by researchers in evaluating the performance of hydrological models [45,46]. When selecting NSE and RE as the objective functions for parameter calibration, the closer the NSE is to 1 and RE to 0, the better the simulation results will be [47]. The objective functions are calculated in Equations (12) and (13):

$$SE = 1 - \frac{\sum_{i=1}^N (Q_i^{obs} - Q_i^{sim})^2}{\sum_{i=1}^N (Q_i^{obs} - Q_{avg}^{obs})^2} \tag{12}$$

$$RE = \frac{|\sum_{i=1}^N Q_i^{obs} - \sum_{i=1}^N Q_i^{sim}|}{\sum_{i=1}^N Q_i^{obs}} \times 100\% \tag{13}$$

where Q_i^{obs} is the observed discharge series (m^3/s), Q_i^{sim} is the simulated discharge series (m^3/s), Q_{avg}^{obs} is the average value of the observed discharge series (m^3/s), N is the length of the discharge series (month), i is the serial number.

4. Results

4.1. Interannual and Seasonal Variations of Hydrometeorological Series in 1973–2014

The areal average temperature and precipitation over the upper Tang River catchment during 1973–2014 are calculated based on the grid data set CN05.1 ($0.25^\circ \times 0.25^\circ$) from CMA. The interannual and seasonal variations of precipitation, air temperature, and runoff series are presented in Figure 3. The MK trend test results of the three series are shown in Table 1, in which the S (the slope coefficient) indicates the magnitude of the series change.

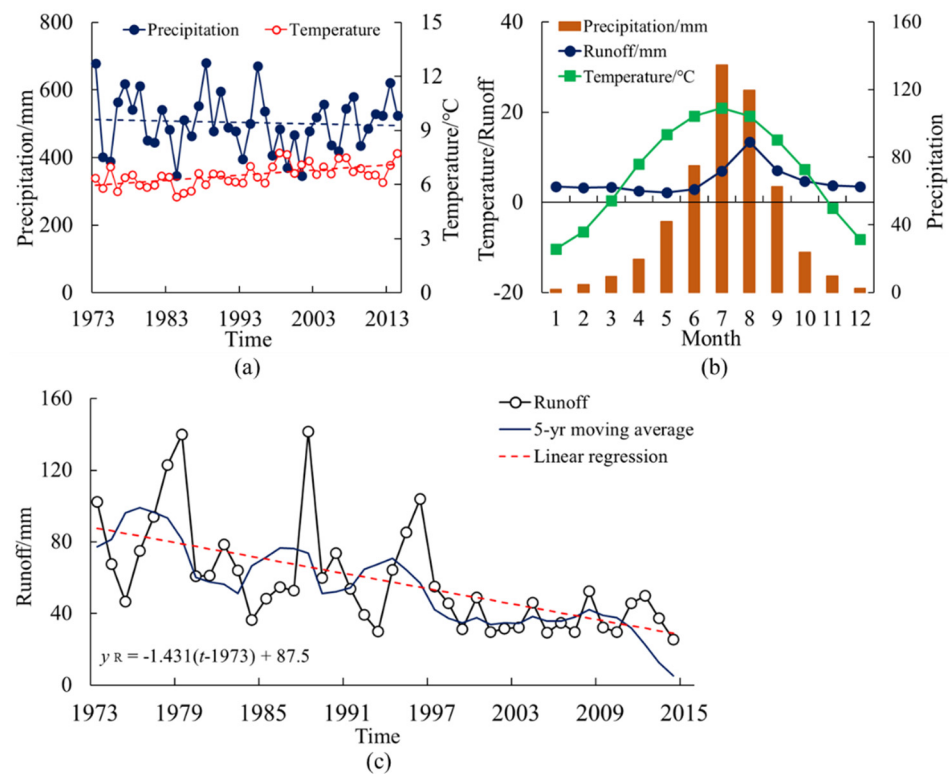


Figure 3. The interannual (a,c) and seasonal (b) variations of precipitation (mm), temperature ($^\circ C$), and runoff (mm) series during 1973–2014 in the upper Tang River catchment.

Table 1. Trend test results of annual precipitation, temperature, and runoff during 1973–2014.

Series	S	Trend	Z_{MK}	Significance
Precipitation	-0.479 mm/year	↓	-0.1734	No
Temperature	$+0.028 \text{ }^\circ C/\text{year}$	↑	3.8364	Yes
Runoff	-1.431 mm/year	↓	-4.4433	Yes

Figure 3 and Table 1 indicate that the downward trend of the observed runoff series from 1973 to 2014 was significant with a linear rate of $-14.31 \text{ mm}/10 \text{ year}$. The interannual variations of runoff series varied widely, with the maximum value being five times the minimum one. There was also an insignificant downward trend in the annual precipitation series (a linear rate of $-4.79 \text{ mm}/10 \text{ year}$) in the upper Tang River catchment, while the upward trend in the air temperature series was significant with a linear rate of $+0.28 \text{ }^\circ C/10 \text{ year}$. The annual precipitation ranged from 345 mm to 680 mm during 1973–2014, with a difference of more than 50% between maximum and minimum values. The maximum

runoff and precipitation both occurred in 1988. The trend analysis revealed that the decrease in precipitation might be the main climate factor of runoff reduction, which would be accelerated by the warmer air temperature. The seasonal variations showed that the distributions of runoff and precipitation in the upper Tang River catchment were extremely uneven, with 78% of precipitation and 53% of runoff concentrating in the flood season (from June to September). Both precipitation and temperature reached their maximum values in July, while runoff reached its maximum value in August due to the effects of environmental delay.

4.2. Mutation Test of Hydrometeorological Series in 1973–2014

The first-order autocorrelation coefficients of precipitation, air temperature, and runoff series are 0.083, 0.205, and 0.312, respectively, with only the runoff series reaching the significance level ($\alpha = 0.05$, $r_\alpha = 0.304$). Therefore, the TFPW method is applied to the observed runoff series to obtain a new detrended series, Runoff_TFPW. Next, abrupt changes in precipitation, air temperature, and runoff series with and without TFPW pretreatment are detected by Mann–Kendall, Pettitt, and Sequential Cluster methods to reduce the uncertainty caused by single mutation test. The results of different mutation tests are summarized in Table 2.

Table 2. Mutation test results of annual precipitation, temperature, and runoff during 1973–2014.

Series	Mann–Kendall	Pettitt	Sequential Cluster
Precipitation	1977, 2013	1979	1973
Temperature	1993	1996	1996
Runoff	1992, 1996	1997	1996
Runoff_TFPW	1996	1996	1996

Table 2 shows that the test results of abrupt changes in annual precipitation series were different by various mutation test methods in the study period. Combining the abrupt changes and long-time variations in precipitation series, it was judged that there was no obvious mutation year of precipitation in the upper Tang River catchment. Both 1993 and 1996 might be the mutation years of the annual temperature series according to the mutation test results, while the jump amount around 1996 (+0.84 °C) was higher than that around 1993 (+0.81 °C), so the abrupt change in the air temperature series was determined as 1996. The TFPW method had a certain correction effect on mutation detection of the observed runoff series. Before removing autocorrelation, the results of the original runoff series by various mutation test methods were not consistent and the abrupt changes could not be judged intuitively. After the removal of autocorrelation by the TFPW method, the abrupt change of runoff_TFPW series unified in 1996. Thus, 1996 was the mutation year in the hydrological and meteorological series of the upper Tang River catchment.

In order to explore the changes in hydrometeorological characteristics before and after the mutation year, the hydrological and meteorological series are divided by 1996, and changes in precipitation, air temperature, and runoff series are summarized in Table 3. Relationships between precipitation and runoff on monthly and annual scales before and after 1996 are shown in Figure 4.

Table 3. Relative changes in precipitation, temperature, and runoff before and after 1996.

Series	1973–1996	1996–2014	Relative Change/%
Precipitation/mm	518.0	484.7	−6.4
Temperature/°C	6.18	7.02	+13.6
Runoff/mm	73.3	38.1	−48.0

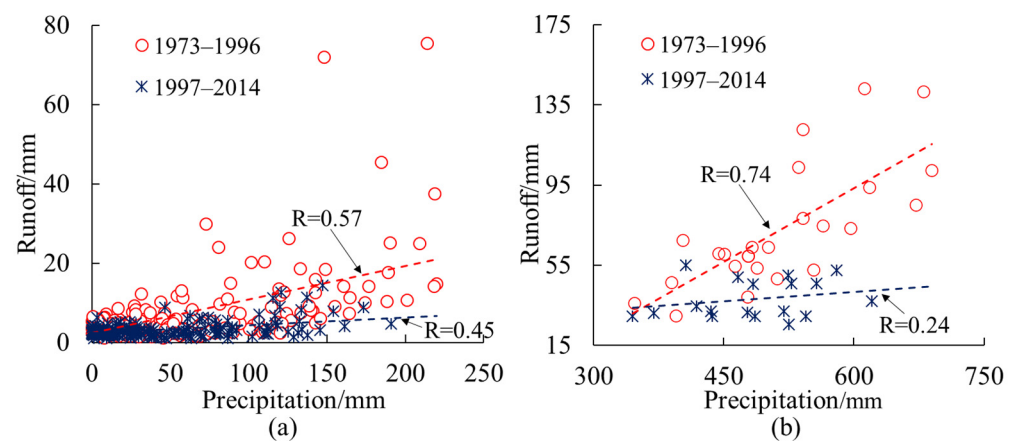


Figure 4. Relationships between precipitation (mm) and runoff (mm) on monthly and annual scales. (a) monthly scale; (b) annual scale.

Figure 4 and Table 3 show that after the mutation year, the annual precipitation and observed runoff decreased by 6.4% and 48%, respectively, while the annual air temperature increased by 12.9%. The correlations between precipitation and runoff reduced significantly after the mutation year both on monthly (0.45–0.57) and annual (0.24–0.74) scales. The precipitation-runoff scattered points moved downward with time, indicating that the runoff generated by similar precipitation continued to decrease. The results showed that precipitation might be the main factor affecting early runoff series in this study catchment. While it came to the later stage, with the intensification of anthropic impacts, e.g., underlying surface changes and groundwater exploitation, the sensitivity of runoff to precipitation gradually decreased in the upper Tang River catchment.

4.3. Periodicity Analysis of Hydrometeorological Series in 1973–2014

Morlet wavelet is a useful tool for the periodicity analysis of hydrological series. It can decompose the sequence and extract the period to reflect variations and trends. Therefore, the Morlet wavelet is applied to the periodicity analysis of precipitation, air temperature, and runoff series. The real part distribution and variance of the Morlet wavelet are shown in Figure 5.

Figure 5 indicates that the annual precipitation in the upper Tang River catchment had periodic characteristics of 7a multiples (7a, 14a, and 21a), with periodic oscillation strongest around 14a and 21a. The annual air temperature exhibited one dominant period of 28a and three sub-dominant periods of 7a, 14a, and 18a. The annual observed runoff had periodic changes on the scales of 8a, 14a, and 21a, among which 14a was the most significant period, followed by 21a and 8a. The periodic changes of precipitation and runoff series were generally consistent, reflecting the influence of precipitation on runoff. The periodic characteristics of the precipitation and temperature series were all-time, while the periods of the runoff series mainly manifested before 1996. After 1996, periodic characteristics on the other two scales gradually disappeared, leaving only the periodic feature of 14a. The periodicity analysis results of the runoff series were consistent with the abrupt changes in mutation tests. Compared with the irregularity of runoff periodicity, the periodic changes in precipitation and temperature series were more stable.

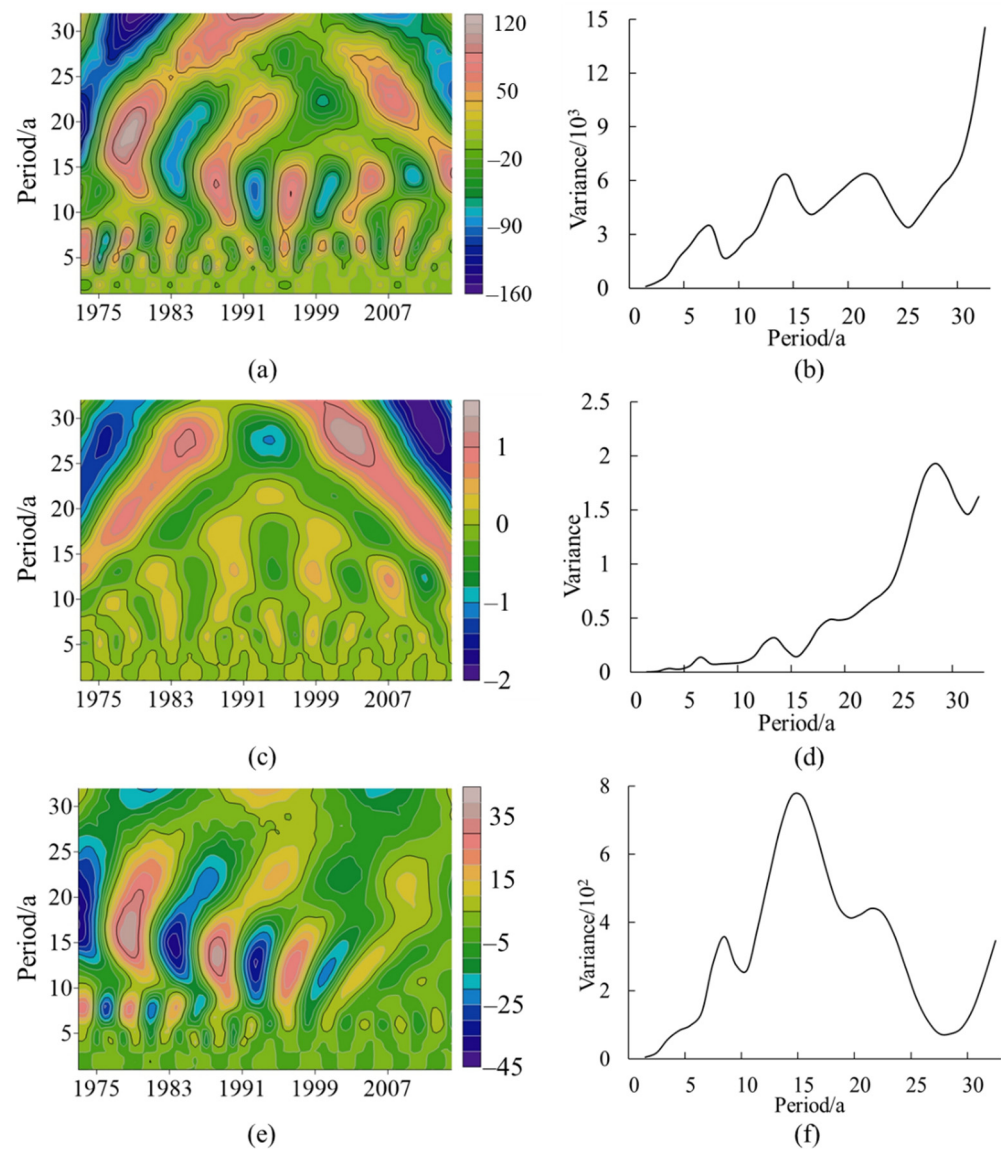


Figure 5. The real part distribution and variance of Morlet wavelet for precipitation (a,b), temperature (c,d), and runoff (e,f) series.

4.4. Hydrological Modeling for Stream Flow in 1973–2014

According to the detection results of the hydrological series in the upper Tang River catchment, the mutation year 1996 is taken as the demarcation point. Before and after 1996, calibration periods and verification periods were selected to investigate hydrological process simulations, respectively. The monthly simulation results of the RCCC-WBM model are presented in Table 4 and Figure 6.

Table 4. Simulated results of the RCCC-WBM model for monthly discharge in the upper Tang River catchment.

Statistics	Before 1996		After 1996	
	Calibration Period (1973–1988)	Verification Period (1989–1996)	Calibration Period (1997–2008)	Verification Period (2009–2014)
NSE	0.74	0.72	0.33	−0.24
RE	−1.24%	−1.32%	−1.12%	21.29%

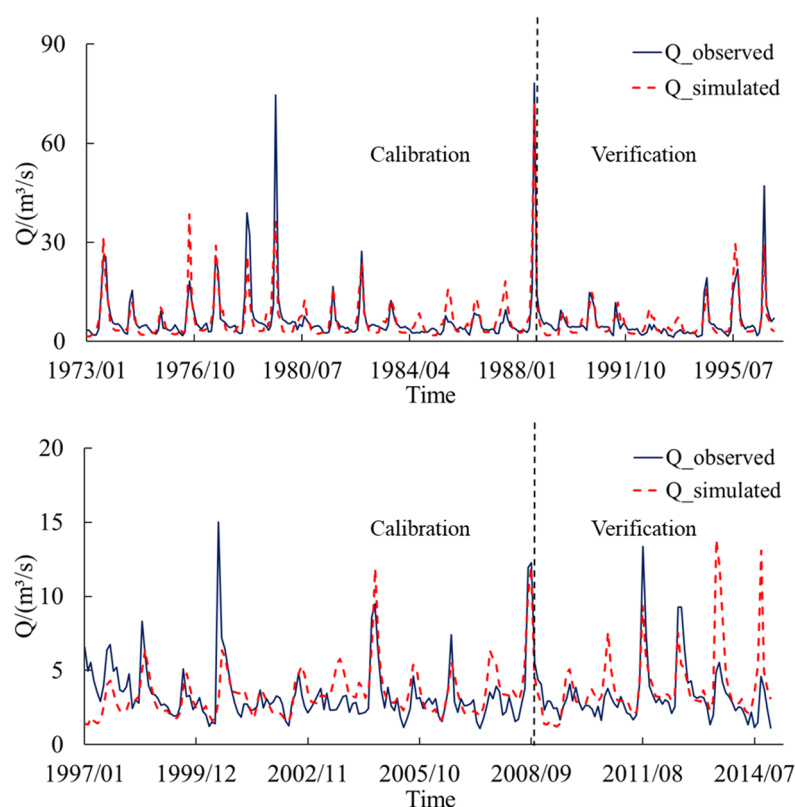


Figure 6. Monthly observed and simulated discharge (m^3/s) before and after 1996 in the upper Tang River catchment.

Table 4 and Figure 6 show that the RCCC-WBM model had a good simulation performance before 1996 in the upper Tang River catchment, with well-fitted observed and simulated discharge since human activities had limited influence on the hydrological cycle. The NSEs both reached 0.70 with calibration period 0.74 and verification period 0.72, and the REs were both controlled within $\pm 3\%$ with calibration period -1.24% and verification period -1.32% , which fully demonstrated the applicability and stability of the RCCC-WBM model during the natural period in this catchment. However, the simulation results were not satisfactory after 1996 with NSE less than 0.35 in the calibration period and even negative in the verification period, but it could still reflect the variations of monthly discharge. The occurrence time of simulated peaks corresponded with the observed ones only in the calibration period before 1996. Next, a time lag between simulated and observed peaks occurred near 1989. The simulated peaks are sometimes significantly lower than the observed ones, which mainly concentrate in flood seasons. For example, the observed discharge in August 1979 is twice the simulated one, and the observed discharge in July 2000 is four times the simulated one. This is mainly because the upper Tang River catchment is located in a semi-arid area with a dry climate and low soil moisture. As a result, the main mechanism of runoff generation is excess infiltration [48]. When rainfall duration is very short and intensity varies greatly, the RCCC-WBM model, as a monthly water balance model, can accurately control water balance, but cannot reflect high-intensity precipitation processes, resulting in larger errors in simulated peaks. After the mutation year (1996), the influence of meteorological factors on the runoff series gradually weakens and the response of runoff to precipitation is complicated by human activities (e.g., groundwater exploitation and agricultural irrigation), resulting in a lower observed discharge compared to the simulated one. For example, the simulated discharge in July 2013 is three times the observed one. Improving the simulation accuracy of hydrological models during periods with intensive human activities in semi-arid regions needs more basic data and remains a challenge to be addressed in the future.

5. Discussion

Previous studies have indicated that the flows of rivers in northern China have decreased to a varying extent due to human activities and climate change in the past 50 years, with the Haihe River being one of the most significant rivers [49–51], which is consistent with the conclusions of this paper. Anthropogenic impacts are the main driving factors for the decrease and mutation of runoff series in northern rivers [52,53]. Meanwhile, variations in precipitation dominate runoff fluctuations, while temperature affects runoff series by changing evaporation [54,55].

The rainfall–runoff process is a comprehensive process affected by many factors, and its formation and evolution are concentrated manifestations of the dual influence of nature and human beings [56]. The main factors affecting runoff fluctuations in northern China are human activities, including water and soil conservation projects, exploitation of groundwater, as well as land cover and use changes [57]. The only large-scale hydraulic project in the Tang River catchment, the Xidayang reservoir, is located downstream of the Daomaguan hydrometric station, and there are no other large water retention structures in the upper Tang River catchment. The catchment is dominated by agriculture and spans two typical industrial cities, Baoding in Hebei province and Datong in Shanxi Province, which is dominated by manufacturing and coal industry, respectively. The farmland is mainly distributed along the river system, so human activities such as water withdrawal for irrigation are frequent. According to statistics, agricultural water in Datong accounts for about 54% of the total water consumption. In some years, such as 2011, the water consumption in Datong (604 million m³) is greater than the total water resources (546 million m³). The contradiction between water supply and demand in Baoding is more prominent. The agricultural water has been about 2.8 billion m³ since 2000, while the total annual water resources in Baoding is only about 2.0 billion m³, which can barely meet the agricultural water demand in some wet years. Agricultural and industrial production requires a large amount of water, but the water resources quantity in the upper Tang River catchment cannot be self-sufficient, so groundwater overexploitation in this area is very common. Most of the groundwater in this catchment is concentrated in river channels of the mountain tributaries, which gives groundwater exploitation good mining conditions and low exploitation costs. The total area of groundwater overexploitation in Datong is 506 km² (the serious overexploitation area is 163 km²), and the accumulated exploitation of groundwater is more than 2.1 billion m³. The groundwater exploitation of Baoding in 2016 is 2.35 billion m³, while the water resources were only 1.57 billion m³ and the exploitation degree of Baoding is 150%. The overexploitation of groundwater leads to a continuous decline in groundwater level and an increase in precipitation infiltration recharge, which is the main reason for runoff reduction in the upper Tang River catchment.

According to the characteristics of the hydrological series in the upper Tang River catchment, the land use data for 1980, 1995, and 2015 are selected to analyze the land-use changes in this area. Figure 7 shows the grassland in the upper Tang River catchment accounts for the largest proportion, about 47.0%, followed by forest and farmland, accounting for 27.0% and 22.6%, respectively. The water body and urban and rural construction land are both less than 3%. The land use of the catchment remained unchanged during 1980–1995, but the influence of human activities gradually increased from 1995 to 2015, with the area of farmland decreasing by 18.3 km², water body decreasing by 1.1 km², and urban and rural construction land increasing by 20.3 km². Urbanization and farmland expansion have aggravated water supply pressure in this catchment, resulting in further reduction of the observed runoff series.

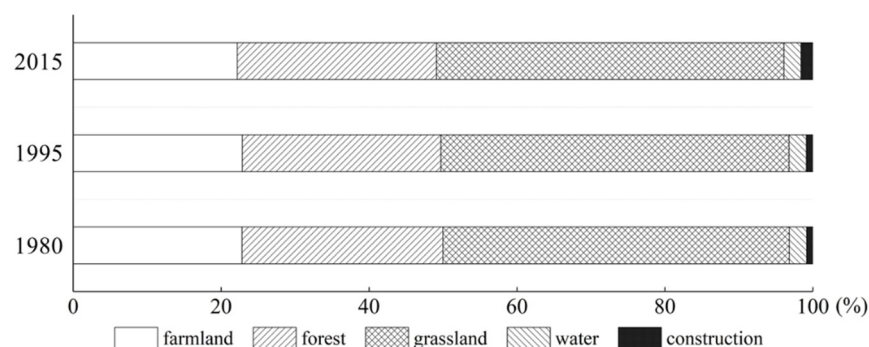


Figure 7. The proportion of land use in the upper Tang River catchment (%).

The eastern route of China's South-to-North Water Diversion Project transports the water resources of the Yangtze River to northern China, which is the largest water diversion project in the world [58]. It can guarantee the ecological flow and improve the situation of water shortage in northern China, but it cannot fundamentally solve the problem of disharmony between economic development and water resources in the Haihe River basin [59]. In recent years, water resources management and water ecological security in the Haihe River basin have gradually received attention, and a series of regulations have been promulgated to address issues such as groundwater overexploitation and water withdrawal for irrigation. At present, the Haihe River basin implements the strictest management system for water resources, which puts forwards requirements on the total water consumption, water use efficiency, and effective utilization coefficient of agricultural water to realize the sustainable use of water resources and support economic and social development in the basin.

6. Conclusions

The analysis of trend, mutation, and periodicity of hydrological series is an active field in statistics, as well as an ongoing concern in hydrology. The annual runoff and precipitation series of the upper Tang River catchment declined at the rate of -0.479 mm/year and -1.431 mm/year, while the upward trend in the annual average temperature series was significant with a linear rate of $+0.028$ °C/year. The distributions of precipitation and runoff were extremely uneven, mainly concentrated in flood seasons (June–September). Temperature and precipitation reached their maximum in July, while runoff reached its maximum in August.

According to the results of various mutation test methods, there was no obvious abrupt change in the precipitation series, and the mutation point of the temperature and runoff series was 1996 for both. Compared with the original series, the runoff series processed by the TFPW method had more unified detection results, and the mutation year was in agreement with Morlet periodicity analysis. Periodicity results of precipitation and runoff series were consistent in the upper Tang River catchment, with periodic changes about 7a multiples (7–8a, 14a, and 21a) and periodic oscillation strongest around 14a. Annual temperature exhibited one dominant period of 28a and three sub-dominant periods.

The RCCC-WBM model performed well for stream flow simulations before the mutation year in the upper Tang River catchment, with the NSEs reaching 0.70 and the REs controlled within $\pm 3\%$. After the mutation year, although the model could still reflect the variations of monthly discharge, the observed flow decreased significantly and the simulation accuracy was not satisfactory due to the influence of anthropogenic activities. Water withdrawal and groundwater exploitation were the main reasons for runoff reduction in this catchment, which is further aggravated by land-use changes such as urbanization and farmland expansion.

The consistency of hydrological series in semi-arid areas has been destroyed under the changing environment, which puts forward higher requirements for the plasticity and

adaptation of hydrological models. How to quantify the impacts of these changes on runoff by using hydrological models will be enhanced in further studies.

Author Contributions: Conceptualization, J.Z., and G.W.; methodology, Y.L.; software, G.W.; validation, Z.B., and Y.Y.; formal analysis, Y.L.; investigation, Y.L.; resources, G.W.; data curation, Y.Y.; writing—original draft preparation, Y.L.; writing—review and editing, Y.L., and G.W.; visualization, Y.L.; supervision, J.Z.; project administration, Z.B.; funding acquisition, G.W. All authors have read and agreed to the published version of the manuscript.

Funding: The study has been financially supported by the National Key Research and Development Programs of China (Grants: 2017YFA0605002), the National Natural Science Foundation of China (Grants: 41830863, 51879162, 52121006, 91847301, 92047203, and 51879164), and the Belt and Road Fund on Water and Sustainability of the State Key Laboratory of Hydrology-Water Resources and Hydraulic Engineering, China (2021490211 and 2020nkzd01). Thanks also to the anonymous reviewers and editors.

Institutional Review Board Statement: Not applicable.

Informed Consent Statement: Not applicable.

Data Availability Statement: Code and data supporting the findings of this study are available from the corresponding author.

Conflicts of Interest: The authors declare no conflict of interest.

References

1. Montanari, A.; Young, G.; Savenije, H.H.G.; Hughes, D.; Wagener, T.; Ren, L.L.; Koutsoyiannis, D.; Cudennec, C.; Toth, E.; Grimaldi, S.; et al. “Panta Rhei—Everything Flows”: Change in hydrology and society—The IAHS Scientific Decade 2013–2022. *Hydrol. Sci. J.* **2013**, *58*, 1256–1275. [[CrossRef](#)]
2. Xue, D.; Zhou, J.; Zhao, X.; Liu, C.; Wei, W.; Yang, X.; Li, Q.; Zhao, Y. Impacts of climate change and human activities on runoff change in a typical arid watershed, NW China. *Ecol. Indic.* **2021**, *121*, 107013. [[CrossRef](#)]
3. Yang, G.; Zhang, M.; Xie, Z.; Li, J.; Ma, M.; Lai, P.; Wang, J. Quantifying the Contributions of Climate Change and Human Activities to Water Volume in Lake Qinghai, China. *Remote Sens.* **2021**, *14*, 99. [[CrossRef](#)]
4. Guo, Q.; Yang, Y.; Xiong, X. Using hydrologic simulation to identify contributions of climate change and human activity to runoff changes in the Kuye river basin, China. *Environ. Earth Sci.* **2016**, *75*, 417. [[CrossRef](#)]
5. Liu, J.; Zhou, Z.; Yan, Z.; Gong, J.; Jia, Y.; Xu, C.; Wang, H. A new approach to separating the impacts of climate change and multiple human activities on water cycle processes based on a distributed hydrological model. *J. Hydrol.* **2019**, *578*, 124096. [[CrossRef](#)]
6. Jin, H.; Rui, X.; Li, X. Analysing the Performance of Four Hydrological Models in a Chinese Arid and Semi-Arid Catchment. *Sustainability* **2022**, *14*, 3677. [[CrossRef](#)]
7. Luo, L.; Zhou, Q.; He, H.S.; Duan, L.; Zhang, G.; Xie, H. Relative Importance of Land Use and Climate Change on Hydrology in Agricultural Watershed of Southern China. *Sustainability* **2020**, *12*, 6423. [[CrossRef](#)]
8. Gao, T.; Xie, L. Spatiotemporal changes in precipitation extremes over Yangtze River basin, China, considering the rainfall shift in the late 1970s. *Glob. Planet. Chang.* **2016**, *147*, 106–124. [[CrossRef](#)]
9. Zhang, A.; Zheng, C.; Wang, S.; Yao, Y. Analysis of streamflow variations in the Heihe River Basin, northwest China: Trends, abrupt changes, driving factors and ecological influences. *J. Hydrol. Reg. Stud.* **2015**, *3*, 106–124. [[CrossRef](#)]
10. Zhou, C.; van Nooijen, R.; Kolechkina, A.; Hrachowitz, M. Comparative analysis of nonparametric change-point detectors commonly used in hydrology. *Hydrol. Sci. J.* **2019**, *64*, 1690–1710. [[CrossRef](#)]
11. Wang, X.; Hou, X.; Wang, Y. Spatiotemporal variations and regional differences of extreme precipitation events in the Coastal area of China from 1961 to 2014. *Atmos. Res.* **2017**, *197*, 94–104. [[CrossRef](#)]
12. Roundy, P.E. Interpretation of the spectrum of eastward-moving tropical convective anomalies. *Q. J. R. Meteorol. Soc.* **2019**, *146*, 795–806. [[CrossRef](#)]
13. Minaei, M.; Irannezhad, M. Spatio-temporal trend analysis of precipitation, temperature, and river discharge in the northeast of Iran in recent decades. *Theor. Appl. Climatol.* **2018**, *131*, 167–179. [[CrossRef](#)]
14. Sonali, P.; Kumar, N.D. Detection and attribution of seasonal temperature changes in India with climate models in the CMIP5 archive. *J. Water Clim. Chang.* **2016**, *7*, 83–102. [[CrossRef](#)]
15. Li, C.; Wu, P.T.; Li, X.L.; Zhou, T.W.; Sun, S.K.; Wang, Y.B.; Luan, X.B.; Yu, X. Spatial and temporal evolution of climatic factors and its impacts on potential evapotranspiration in Loess Plateau of Northern Shaanxi, China. *Sci. Total Environ.* **2017**, *589*, 165–172. [[CrossRef](#)] [[PubMed](#)]
16. Dashtpajardi, M.M.; Kousari, M.R.; Vagharfard, H.; Ghonchepour, D.; Hosseini, M.E.; Ahani, H. An investigation of drought magnitude trend during 1975–2005 in arid and semi-arid regions of Iran. *Environ. Earth Sci.* **2014**, *73*, 1231–1244. [[CrossRef](#)]

17. Mallick, J.; Talukdar, S.; Alsubih, M.; Salam, R.; Ahmed, M.; Ben, K.N.; Shamimuzzaman, M. Analysing the trend of rainfall in Asir region of Saudi Arabia using the family of Mann-Kendall tests, innovative trend analysis, and detrended fluctuation analysis. *Theor. Appl. Climatol.* **2020**, *143*, 823–841. [[CrossRef](#)]
18. Liu, D.; Mishra, A.K.; Ray, D.K. Sensitivity of global major crop yields to climate variables: A non-parametric elasticity analysis. *Total Environ.* **2020**, *748*, 141431. [[CrossRef](#)]
19. George, Z.N.; Yali, E.W. Evaluation of Streamflow under Climate Change in the Zambezi River Basin of Southern Africa. *Water* **2021**, *13*, 3114. [[CrossRef](#)]
20. Zhang, Y.; Wu, Z.; Singh, V.P.; Su, Q.; He, H.; Yin, H.; Zhang, Y.; Wang, F. Simulation of Crop Water Demand and Consumption Considering Irrigation Effects Based on Coupled Hydrology-Crop Growth Mode. *J. Adv. Model. Earth Syst.* **2021**, *13*, e2020MS002360. [[CrossRef](#)]
21. Zhou, Z.; Jia, Y.; Qiu, Y.; Liu, J.; Wang, H.; Xu, C.; Li, J.; Liu, L. Simulation of Dualistic Hydrological Processes Affected by Intensive Human Activities Based on Distributed Hydrological Model. *J. Water Resour. Plan. Manag.* **2018**, *144*, 04018077. [[CrossRef](#)]
22. Zocatelli, D.; Marra, F.; Smith, J.; Goodrich, D.; Unkrich, C.; Rosensaft, M.; Morin, E. Hydrological modelling in desert areas of the eastern Mediterranean. *J. Hydrol.* **2020**, *587*, 124879. [[CrossRef](#)]
23. Hosseini, S.H.; Khaleghi, M.R. Application of SWAT model and SWAT-CUP software in simulation and analysis of sediment uncertainty in arid and semi-arid watersheds (case study: The Zoshk–Abardeh watershed). *Model. Earth Syst. Environ.* **2020**, *6*, 2003–2013. [[CrossRef](#)]
24. Xu, C.Y. Issues influencing accuracy of hydrological modeling in a changing environment. *Water Sci. Eng.* **2021**, *14*, 167–170. [[CrossRef](#)]
25. Xu, H.; Ren, Y.; Zheng, H.; Ouyang, Z.; Jiang, B. Analysis of Runoff Trends and Drivers in the Haihe River Basin, China. *Int. J. Environ. Res. Public Health* **2020**, *17*, 1577. [[CrossRef](#)] [[PubMed](#)]
26. Yang, X.; Sun, W.; Mu, X.; Gao, P.; Zhao, G. Runoff affected by climate and anthropogenic changes in a large semi-arid river basin. *Hydrol. Process.* **2020**, *34*, 1906–1919. [[CrossRef](#)]
27. Wu, L.; Zhang, X.; Hao, F.; Wu, Y.; Li, C.; Xu, Y. Evaluating the contributions of climate change and human activities to runoff in typical semi-arid area, China. *J. Hydrol.* **2020**, *590*, 125555. [[CrossRef](#)]
28. Umar, D.A.; Ramli, M.F.; Aris, A.Z.; Jamil, N.R.; Abdulkareem, J.H. Runoff irregularities, trends, and variations in tropical semi-arid river catchment. *J. Hydrol. Reg. Stud.* **2018**, *19*, 335–348. [[CrossRef](#)]
29. Chinnaamy, P.; Maske, A.B.; Honap, V.; Chaudhary, S.; Agoramoorthy, G. Sustainable development of water resources in marginalised semi-arid regions of India: Case study of Dahod in Gujarat, India. *Nat. Resour. Forum* **2021**, *45*, 105–119. [[CrossRef](#)]
30. He, Y.; Jiang, X.; Wang, N.; Zhang, S.; Ning, T.; Zhao, Y.; Hu, Y. Changes in mountainous runoff in three inland river basins in the arid Hexi Corridor, China, and its influencing factors. *Sustain. Cities Soc.* **2019**, *50*, 101703. [[CrossRef](#)]
31. Martinsen, G.; Liu, S.; Mo, X.; Bauer-Gottwein, P. Joint optimization of water allocation and water quality management in Haihe River basin. *Sci. Total Environ.* **2018**, *654*, 72–84. [[CrossRef](#)] [[PubMed](#)]
32. Bao, Z.; Zhang, J.; Yan, X.; Wang, G.; He, R.; Guan, T.; Liu, C. Quantitative assessment of the attribution of runoff change caused by four factors in the Haihe River basin. *Adv. Water Sci.* **2021**, *32*, 171–181. (In Chinese) [[CrossRef](#)]
33. Darshana, P.A.; Pandey, R.P. Analysing trends in reference evapotranspiration and weather variables in the Tons River Basin in Central India. *Stoch. Environ. Res. Risk Assess.* **2013**, *27*, 1407–1421. [[CrossRef](#)]
34. Mann, H.B. Nonparametric tests against trend. *Econometrica* **1945**, *13*, 245–259. [[CrossRef](#)]
35. Kendall, M.G. Rank Correlation Methods. *Br. J. Psychol.* **1990**, *25*, 86–91. [[CrossRef](#)]
36. Wu, C.; Ji, C.; Shi, B.; Wang, Y.; Gao, J.; Yang, Y.; Mu, J. The impact of climate change and human activities on streamflow and sediment load in the Pearl River basin. *Int. J. Sediment Res.* **2019**, *34*, 307–321. [[CrossRef](#)]
37. Pakalidou, N.; Karacosta, P. Study of very long-period extreme precipitation records in Thessaloniki, Greece. *Atmos. Res.* **2018**, *208*, 106–115. [[CrossRef](#)]
38. Hu, S.; Feng, F.; Liu, W.; She, D. Changes in temporal inequality and persistence of precipitation over China during the period 1961–2013. *Hydrol. Res.* **2018**, *49*, 1283–1291. [[CrossRef](#)]
39. Pettitt, A.N. A Non-Parametric Approach to the Change-Point Problem. *J. R. Stat. Soc. Ser. C (Appl. Stat.)* **1979**, *28*, 126–135. [[CrossRef](#)]
40. Ding, J. Statistics detection for transition point in flood time sequences. *Eng. J. Wuhan Univ.* **1986**, *5*, 36–41. (In Chinese)
41. Ma, Z.; Kang, S.; Zhang, L.; Tong, L.; Su, X. Analysis of impacts of climate variability and human activity on streamflow for a river basin in arid region of northwest China. *J. Hydrol.* **2008**, *352*, 239–249. [[CrossRef](#)]
42. Sun, L.; Wang, Y.; Zhang, J.; Yang, Q.; Bao, Z.; Guan, X.; Guan, T.; Chen, X.; Wang, G. Impact of environmental change on runoff in a transitional basin: Tao River Basin from the Tibetan Plateau to the Loess Plateau, China. *Adv. Clim. Chang. Res.* **2019**, *10*, 214–224. [[CrossRef](#)]
43. Wang, G.; Zhang, J.; He, R.; Liu, C.; Ma, T.; Bao, Z.; Liu, Y. Runoff sensitivity to climate change for hydro-climatically different catchments in China. *Stoch. Environ. Res. Risk Assess.* **2016**, *31*, 1011–1021. [[CrossRef](#)]
44. Guan, X.; Zhang, J.; Elmahdi, A.; Li, X.; Liu, J.; Liu, Y.; Jin, J.; Liu, Y.; Bao, Z.; Liu, C.; et al. The Capacity of the Hydrological Modeling for Water Resource Assessment under the Changing Environment in Semi-Arid River Basins in China. *Water* **2019**, *11*, 1328. [[CrossRef](#)]

45. Nash, J.E.; Sutcliffe, J. River flow forecasting through conceptual models: Part 1—A discussion of principles. *J. Hydrol.* **1970**, *10*, 282–290. [[CrossRef](#)]
46. Roostaee, M.; Deng, Z. Effects of Digital Elevation Model Resolution on Watershed-Based Hydrologic Simulation. *Water Resour. Manag.* **2020**, *34*, 2433–2447. [[CrossRef](#)]
47. Liu, Y.; Zhang, J.; Elmahdi, A.; Yang, Q.; Guan, X.; Liu, C.; He, R.; Wang, G. Transferability of the xin'anjiang model based on similarity in climate and geography. *Water Sci. Technol. Water Supply* **2021**, *21*, 2191–2201. [[CrossRef](#)]
48. Huang, P.; Li, Z.; Chen, J.; Li, Q.; Yao, C. Event-based hydrological modeling for detecting dominant hydrological process and suitable model strategy for semi-arid catchments. *J. Hydrol.* **2016**, *542*, 292–303. [[CrossRef](#)]
49. Bu, J.; Lu, C.; Niu, J.; Gao, Y. Attribution of Runoff Reduction in the Juma River Basin to Climate Variation Direct Human Intervention and Land Use Change. *Water* **2018**, *10*, 1775. [[CrossRef](#)]
50. Yang, S.; Kang, T.; Bu, J.; Chen, J.; Wang, Z.; Gao, Y. Detection and Attribution of Runoff Reduction of Weihe River over Different Periods during 1961–2016. *Water* **2020**, *12*, 1416. [[CrossRef](#)]
51. Li, R.; Zheng, H.; Huang, B.; Xu, H.; Li, Y. Dynamic Impacts of Climate and Land-Use Changes on Surface Runoff in the Mountainous Region of the Haihe River Basin, China. *Adv. Meteorol.* **2018**, *2018*, 3297343. [[CrossRef](#)]
52. Wei, Q.; Sun, C.; Wu, G.; Pan, L. Haihe River discharge to Bohai Bay, North China: Trends, climate, and human activities. *Hydrol. Res.* **2017**, *48*, 1058–1070. [[CrossRef](#)]
53. Cheng, X.; Chen, L.; Sun, R.; Kong, P. Land use changes and socio-economic development strongly deteriorate river ecosystem health in one of the largest basins in China. *Total Environ.* **2018**, *616–617*, 376–385. [[CrossRef](#)] [[PubMed](#)]
54. Xu, J.; Gao, X.; Yang, Z.; Xu, T. Trend and Attribution Analysis of Runoff Changes in the Weihe River Basin in the Last 50 Years. *Water* **2021**, *14*, 47. [[CrossRef](#)]
55. Kabir, R.; John, W.; Pomeroy, P.H.W. The sensitivity of snow hydrology to changes in air temperature and precipitation in three North American headwater basins. *J. Hydrol.* **2022**, *606*, 127460. [[CrossRef](#)]
56. Wang, G.; Zhang, J.; Li, X.; Bao, Z.; Liu, Y.; Liu, C.; He, R.; Luo, J. Investigating causes of changes in runoff using hydrological simulation approach. *Appl. Water Sci.* **2017**, *7*, 2245–2253. [[CrossRef](#)]
57. Xu, F.; Jia, Y.; Niu, C.; Sobkowiak, L.; Zhao, L. Evaluating spatial differences in the contributions of climate variability and human activity to runoff change in the Haihe River basin. *Hydrol. Sci. J.* **2021**, *66*, 2060–2073. [[CrossRef](#)]
58. Liu, J.; Li, M.; Wu, M.; Luan, X.; Wang, W.; Yu, Z. Influences of the south-to-north water diversion project and virtual water flows on regional water resources considering both water quantity and quality. *J. Clean. Prod.* **2020**, *244*, 118920. [[CrossRef](#)]
59. Kattel, G.R.; Shang, W.; Wang, Z.; Langford, J. China's South-to-North Water Diversion Project Empowers Sustainable Water Resources System in the North. *Sustainability* **2019**, *11*, 3735. [[CrossRef](#)]